

1 **Exploring the use of spray congealing to produce solid dispersions**
2 **with enhanced indomethacin bioavailability: *in vitro* characterization**
3 **and *in vivo* study**

4
5 Serena Bertoni¹, Beatrice Albertini¹, Luca Ferraro², Sarah Beggiato²,

6 Alessandro Dalpiaz^{3*}, Nadia Passerini^{1*}

7
8
9 ¹*Department of Pharmacy and BioTechnology, PharmTech Lab, University of Bologna,*

10 *Via S. Donato 19/2, 40127 Bologna, Italy,*

11 ²*Department of Life Sciences and Biotechnology, University of Ferrara, via L. Borsari 46, 44121, Ferrara,*
12 *Italy*

13 ³*Department of Chemical and Pharmaceutical Sciences, University of Ferrara, Via Fossato di Mortara 19,*
14 *44121 Ferrara, Italy*

15
16
17
18 *Corresponding authors:

19 Prof. Nadia Passerini

20 Phone: +39-0512095613

21 email: nadia.passerini@unibo.it

22
23 [Prof. Alessandro Dalpiaz](#)

24 email: dla@unife.it

25

26

27 **Abstract**

28 The current study proposes an original oral delivery system for the bioavailability enhancement of
29 indomethacin (IND), a BCS class II drug, with the aim to overcome the common limitations of
30 amorphous solid dispersion. In fact, the potential risk of drug re-crystallization is a serious concern
31 for the stability of amorphous systems and represents, despite the great bioavailability, one of the
32 primary causes of their limited clinical applications. IND-loaded microparticles (MPs) were
33 prepared by spray congealing using oral-approved excipients (Gelucire 50/13 and the recently
34 marketed Gelucire 48/16). MPs were characterized regarding particle size, morphology, drug
35 content and IND solid state; moreover, they were tested *in vitro* for IND solubility and dissolution
36 rate. Solid state characterization indicated that IND was present into the MPs in the amorphous
37 form. The best formulation showed a considerable enhancement in drug dissolution rate and 31-fold
38 higher drug solubility than pure γ -IND. The oral administration of MPs showed 2.5-times increased
39 bioavailability *in vivo* compared to either pure γ -IND or its physical mixture with unloaded MPs.
40 Notably, the formulation was stable after 18 months with no changes in IND solid state and
41 dissolution performance. This study offers a valid approach to enhance IND oral bioavailability by
42 conversion into the amorphous form by spray congealed MPs, which have great potential for
43 industrial application due to their characteristics of high encapsulation efficiency, no-toxicity, low-
44 cost, prolonged stability and the use of a simple and easily scaled-up manufacturing technology.

45

46 **Keywords:** spray congealing, indomethacin, solid dispersion, microparticles, oral bioavailability,
47 poorly soluble drug.

48

50 **1. Introduction**

51 The preparation of Solid Dispersion (SD) is one of the most commonly used approach to improve
52 the biopharmaceutical properties of drugs belonging to class II of the Biopharmaceutical
53 Classification System (BCS) [1] [2] [3]. In SD the drug is incorporated in an inert hydrophilic
54 carrier in the solid state. The success of SD lies in the potential to (i) decrease the drug particle size
55 even up to molecular level (ii) modify the drug solid state from a thermodynamically stable form to
56 a high-energy one and (iii) improve drug particles wettability by the aid of the hydrophilic
57 excipient. However, various problems limit SD industrial applications. Specifically, the low
58 reproducibility and consistency in the quality of SD often lead to variations in the bioavailability
59 [4]. In addition, due to the intrinsic characteristics of SD, the physico-chemical instability of the
60 dosage form during manufacturing and storage is probably the main issue that still need to be totally
61 addressed [5]. For the aforementioned reasons, managing the commercial production of SD-based
62 products is more challenging than traditional products containing drugs in their most stable solid
63 form [6]. [The methods for the preparation of SD can be categorized in three types: solvent-based
64 methods \(e.g. spray drying, freeze-drying\), melting-based methods \(e.g. hot melt extrusion\) and the
65 recently introduced mechanochemical activation, based on high energy milling techniques \(e.g.
66 cryo-milling\) \[7\].](#) An important reason of concerns in view of an industrial application of SD is the
67 toxicity related with the use of organic solvents. On the other hand, the melting-based methods also
68 presents some drawbacks, such as need of multiple downstream processes and, thus, higher
69 production costs. [The mechanochemical activation leads to products with unfavourable handling
70 characteristics \(i.e. poor flowability\).](#) Therefore, there is increasing need of simple, inexpensive
71 technologies for the production of stable SD.

72 Indomethacin (IND) is a non-steroidal anti-inflammatory drug, belonging to BCS class II, used for
73 the treatment of rheumatoid arthritis and other chronic inflammatory diseases. Despite its long time

74 and widespread use [8], IND can cause severe gastrointestinal complications, increased blood
75 pressure and decreased kidney function [9], and the risk of developing these adverse effects
76 increases in the case of high doses and prolonged treatments. Additionally, the poor water solubility
77 of IND represents a major limitation for its oral bioavailability. Many attempts to increase IND
78 solubility and dissolution rate using different formulation strategies have been reported [9] [10] [11]
79 [12], with the ultimate objective of reducing the daily dose and/or administration frequency.

80 This research proposes an original oral delivery system for the bioavailability enhancement of IND,
81 which can address the multiple demands, desirable for a successful SD, of reproducible *in vitro* and
82 *in vivo* performance, easily scaled-up manufacturing technology, non-toxic and low-cost
83 formulation and prolonged stability. Specifically, spray congealing technology was used for the
84 manufacturing of IND-containing SD in the form of microparticles (MPs). Spray congealing is a
85 technology commonly used for the encapsulations of nutrients and drugs mainly in the food and
86 veterinary industries. The process is based on the atomization of a fluid, consisting in a solution or
87 suspension of a drug in a molten carrier, and on the subsequent solidification of the “spray”. The
88 result consists in solid, highly spherical MPs with very good flowing properties and ready-to-use
89 [13]. A commercially available mixtures of mono, di and triglycerides with PEG esters of fatty
90 acids, called “Gelucires” were chosen as hydrophilic low-melting temperature carriers. Gelucires
91 are a family of vehicle including different excipients, all Generally Recognized as Safe (GRAS) and
92 oral-approved, wherein Gelucire 50/13 is probably the most studied for preparing matrix system
93 such as particles, granules [14], minitablets [15] and solid dispersions [16] and successfully used in
94 spray congealing [17]. In this study Gelucire 48/16, a new excipient recently marketed, was
95 evaluated as suitable carrier to prepare MPs by means of spray congealing. Hence, the initial focus
96 of our research was to explore the potential of Gelucire 48/16 for the dissolution enhancement of
97 IND and compare it to Gelucire 50/13. Being SD complex binary systems where each component
98 might influence the behaviour of the other, the physicochemical properties of both components may
99 determine the overall performance of the final formulation [18]. Therefore, a detailed solid state

100 characterization was performed to understand the physicochemical properties of IND-loaded MPs
101 after manufacturing and during storage. *In vitro* investigation on the MPs biopharmaceutical
102 properties and *in vivo* study on rats after oral administration were performed to assess the benefits
103 of the proposed formulation on oral bioavailability. Finally, the long-term stability of the best
104 formulation for more than a year was evaluated.

105

106 **2. Material and methods**

107 **Materials**

108 Gelucire 50/13 and Gelucire 48/16 were kindly supplied from Gattefossè (Milan, Italy). γ -
109 Indomethacin (γ -IND), 9-phenyl-carbazole, phosphoric acid and absolute ethanol were obtained
110 from Sigma Aldrich (Steinheim, Germany). Methanol and water were high performance liquid
111 chromatography (HPLC) grade from Sigma Aldrich (Milan, Italy). All other reagents and solvents
112 were of analytical grade (Sigma-Aldrich). Male Sprague–Dawley rats were provided by Charles-
113 River (Milan, Italy).

114 **Preparation of IND-loaded MPs**

115 MPs were produced by spray congealing using an external-mix two-fluid atomizer, called Wide
116 Pneumatic Nozzle (WPN). Initially, the excipients of the formulation (Gelucire 50/13 and Gelucire
117 48/16 in different ratio) were heated up to a temperature 5 °C above their melting point. IND (10%
118 w/w) was added to the molten carrier and magnetically stirred until complete solubilization, and
119 then loaded into the feeding tank. The temperature of the feeding tank of the nozzle and the inlet air
120 pressure were set at 65°C and 3.5 bar, respectively. The atomized molten droplets hardened during
121 the fall into a cylindrical cooling chamber, which was held at room temperature and the MPs were
122 collected from the bottom of the cooling chamber. Three different drug-loaded formulations (MPs
123 A, MPs B, MPs C) were produced (**Table 1**). For comparison purposes, physical mixes of γ -IND

124 and excipients in the same weight ratio as the loaded MPs were prepared by mixing 10% of γ -IND
125 with 90% of unloaded MPs.

126

127 **IND-loaded MPs characterization**

128 *Morphological analysis.* Shape and surface morphology of IND and MPs were observed by
129 Scanning Electron Microscopy (SEM). Samples were fixed on the sample holder with double-sided
130 adhesive tape, sputter coated with Au/Pd under argon atmosphere performed using a vacuum
131 evaporator (Edwards, Crawley UK) and examined by means of a scanning electron microscope
132 (ESEM Quanta-200) operating at 20,0 kV accelerating voltage.

133 *Particle size analysis.* Size distribution of MPs was evaluated by sieve analysis using a vibrating
134 shaker (Octagon Digital, Endecotts, London UK) and a set of six sieves ranging from 75 to 500 μm
135 (Scientific Instrument, Milan, Italy).

136 *Determination of drug content.* IND content was determined by dissolving 20 mg of MPs accurately
137 weighed in 50 mL of ethanol. The solution was shaken for 24h at 25°C. Finally, the solution was
138 filtered, diluted with the same solvent, and the drug content was assayed spectrophotometrically
139 (UV2 Spectrometer, Unicam) at 320 nm. Each formulation was analysed in triplicate and the mean
140 \pm SD was reported.

141 *Differential scanning calorimetry (DSC) studies.* DSC analysis were performed using a Perkin
142 Elmer DSC 6 (Perkin Elmer, Beaconsfield UK) with nitrogen as purge gas (20mL/min). The
143 instrument was calibrated with indium and lead for temperature, and with indium for the
144 measurements of the enthalpy. Samples of pure IND, unloaded MPs and IND-loaded MPs,
145 weighing 8-9 mg, were placed in an aluminium pan and heated from 25 to 220°C at a scanning rate
146 of 10°C/min.

147 *Fourier transform-infrared spectra (FT-IR) analysis.* Studies of infrared spectra of pure drug,
148 unloaded MPs and IND-loaded MPs were conducted with an IR spectrophotometer (Jasco FT-IR A-
149 200) using the KBr disc method. The samples were mixed with KBr and compressed into tablet
150 (10mm in diameter and 1 mm in thickness) using an hydraulic press (Perkin Elmer, Norwalk USA).
151 The scanning range was 650-4000 cm^{-1} and the resolution was 1 cm^{-1} .

152 *Hot Stage Microscopy (HSM) analysis.* Physical changes in the samples during heating were
153 monitored by HSM studies using a hot stage apparatus (Mettler-Toledo S.p.A., Novate Milanese,
154 Italy) mounted on Nikon Eclipse E400 optical microscope connected to a Nikon Digital Net Camera
155 DN100 for the image acquisition. The samples were equilibrated 25°C for 1 min and then heated at
156 a scanning rate of 10°C/min in the 25-200°C range of temperature. The magnification was set at
157 10x.

158 *Powder X-Ray Diffraction (PXRD) analysis.* Single components, MPs and corresponding physical
159 mixtures were studied by X-ray powder diffraction technique using a Philips X'Pert powder
160 diffractometer equipped with a graphite monochromator in the diffracted beam. $\text{CuK}\alpha$ radiation was
161 used (40 mA, 40 kV). The spectra had been obtained in the 3°–35° 2θ range using a 0.05° step and a
162 0.216°/s speed.

163 **Solubility and dissolution studies**

164 Solubility measurements of pure IND and of IND-loaded MPs were performed in 10 mL of
165 phosphate buffer (0.2 M, pH 5.8) at 25°C. The samples were magnetically stirred for 48h,
166 equilibrated for 2h and the suspensions were then centrifuged at 10.000 rpm for 10 minutes. The
167 supernatant was filtered through a 0.20 μm membrane filter. Finally, the filtrates were suitably
168 diluted with the same solvent and analysed at 266 nm by UV-Visible spectrophotometer. The study
169 was performed in triplicate.

170 A dissolution paddle apparatus (Pharmatest, Steinheim, Germany) was used with a stirring rate of
171 50 rpm. The dissolution medium (phosphate buffer 0.2 M, pH 5.8) was maintained at a temperature
172 of 37°C. Samples of IND, physical mixtures and IND-loaded MPs (size fraction 100-150 µm)
173 containing a suitable amount of IND for sink conditions ($C < 0.2 C_s$) were added to 500 mL of
174 dissolution medium. The aqueous solution was filtered and continuously pumped (12.5 mL/min) to
175 a flow cell in a spectrophotometer (UV2 Spectrometer, Unicam) and absorbance values were
176 recorded at 266 nm. The dissolution tests were performed in triplicate. Dissolution profiles were
177 individually compared using the “similarity factor, f_2 ”, which could be defined as follows:

$$f_2 = 50 * \log \left\{ 1 + \left[\frac{1}{n} * \sum_{t=1}^n (R_t - T_t)^2 \right]^{-0.5} * 100 \right\}$$

178
179 Where n is the sample number, R_t and T_t are the reference assay and test assay at time point t ,
180 respectively.

181 **In Vivo Studies**

182 *HPLC Analysis.* The IND quantification for bioavailability studies was performed by HPLC. The
183 chromatographic apparatus consisted of a modular system (model LC-10 AD VD pump and model
184 SPD- 10A VP variable wavelength UV–vis detector; Shimadzu, Kyoto, Japan) and an injection
185 valve with 20 µL sample loop (model 7725; Rheodyne, IDEX, Torrance, CA, USA). Separation
186 was performed at room temperature on a reverse phase column Hypersil BDS C-18, 5U, equipped
187 with a guard column packed with the same Hypersil material (Alltech Italia Srl BV, Milan, Italy).
188 Data acquisition and processing were accomplished with a personal computer using CLASS-VP
189 Software, version 7.2.1 (Shimadzu Italia, Milan, Italy). The detector was set at 319 nm. The mobile
190 phase consisted of a mixture of methanol and 0.2% phosphoric acid (75:25 v/v). The flow rate was
191 1 mL/min. The compound 9-phenyl-carbazole was used as internal standard in extraction
192 procedures of IND from rat blood (see below). The retention times for IND and 9-phenyl-carbazole
193 were 3.9 and 14.7 minutes, respectively.

194 The chromatographic precision for each compound was evaluated by repeated analysis ($n = 6$) of
195 the same samples. For IND and 9-phenyl-carbazole dissolved in mobile phase the values were
196 obtained for 50 μM (0.018 mg/mL and 0.012 mg/mL, respectively) solutions and were represented
197 by the relative standard deviation (RSD) values ranging between 0.61% and 0.72%, respectively.
198 The efficacy of IND extraction from blood samples was determined by recovery experiments,
199 comparing the peak areas extracted from 10 μM (3.6 $\mu\text{g/mL}$) blood test samples at 4° C with those
200 obtained by injection of an equivalent concentration of the drug dissolved in their mobile phase.
201 The average recovery \pm SD of IND from rat blood resulted $85.8 \pm 3.6\%$. The concentrations of this
202 compound were therefore referred to as peak area ratio with respect to the internal standard 9-
203 phenyl-carbazole. The precision of the method based on peak area ratio, calculated for 10 μM (3.6
204 $\mu\text{g/mL}$) solutions, was represented by RSD values of 0.91%. The calibration of IND was performed
205 by using nine different concentrations in whole blood at 4 °C ranging from 2 μM (0.72 $\mu\text{g/mL}$) to
206 80 μM (28.6 $\mu\text{g/mL}$) and expressed as peak area ratios of the compounds to the internal standard
207 versus concentration. The calibration curve resulted linear ($n = 9$, $r = 0.992$, $P < 0.0001$).

208

209 *In Vivo Administration of Indomethacin: Intravenous Infusion.* Male Sprague Dawley rats (200–250
210 g; $n = 4$), received a femoral intravenous infusion (0.2 mL/min for 5 min) of 0.90 mg/mL
211 indomethacin dissolved in a medium constituted by 20% (v/v) DMSO and 80% (v/v) physiologic
212 solution. At the end of infusion and at fixed time points within 24 hours, blood samples (300 μL)
213 were collected and inserted in heparinized test tubes that were centrifuged at 4°C for 15 min at
214 1,500 x g; 100 μL of plasma were then withdrawn and immediately quenched in 300 μL of ethanol
215 (4 °C); 100 μL of internal standard (100 μM 9-phenyl-carbazole dissolved in ethanol) was then
216 added. After centrifugation at 13,000 x g for 10 min, 400 μL aliquots were reduced to dryness under
217 a nitrogen stream and stored at -20° C until analysis. The samples were dissolved in 150 μL of
218 mobile phase (methanol and 0.2% phosphoric acid 75:25 v/v), and, after centrifugation, 10 μL was

219 injected into the HPLC system for IND assay. All the values obtained were the mean of four
220 independent experiments. The *in vivo* half-life of IND in the blood was calculated by nonlinear
221 regression (exponential decay) of concentration values in the time range within 24 hours after
222 infusion and confirmed by linear regression of the log concentration values *versus* time. The area
223 under the concentration-time curve (AUC) value was calculated by the trapezoidal method within
224 24 hours, the remaining area was determined as the ratio between the indomethacin concentration
225 detected at 24 hour and the elimination constant (k_{el}), that was obtained from the slope of the
226 semilogarithmic ($-\text{slope} \cdot 2.3$). All the calculations were performed by using the computer program
227 Graph Pad Prism.

228

229 *In Vivo Administration: Oral Administration of Indomethacin.* Powders constituted by γ -IND, or its
230 physical mixture with unloaded MPs C or by IND-loaded MPs C were mixed with palatable food in
231 order to induce their oral assumption by male Sprague Dawley rats (200–250 g; n = 4/group) fasted
232 for 24 hours. The dose of orally administered IND was 2 mg for each type of powders. At the end
233 of administration at fixed time points within 8 hours, blood samples (300 μ L) were collected, then
234 extracted and analyzed as above described.

235 All *in vivo* experiments were performed in accordance with the European Communities Council
236 Directive of September 2010 (2010/63/EU), a revision of Directive 86/609/EEC, the Declaration of
237 Helsinki, and the Guide for the Care and Use of Laboratory Animals as adopted and promulgated
238 by the National Institutes of Health (Bethesda, Maryland, USA). The protocol of all the *in vivo*
239 experiments was approved by the Local Ethics Committee (University of Ferrara, Ferrara, Italy).
240 Efforts were made to reduce the number of the animals and their suffering.

241 The AUC values referred to each orally administered treatment were calculated by the trapezoidal
242 method within 8 hours, the remaining area was determined as the ratio between the indomethacin
243 concentration detected at 8 hour and the elimination constant (k_{el}). The absolute bioavailability
244 values of IND, referred to the oral administered samples, were obtained as the ratio between their

245 oral AUC values and AUC of the intravenous administration of the drug, normalized with respect
246 to their doses, according to the following equation [19]:

$$247 \quad F = \frac{AUC_{oral} \cdot dose_{IV}}{AUC_{IV} \cdot dose_{oral}}$$

248 All the calculations were performed by using the computer program Graph Pad Prism.

249

250 **Stability studies**

251 After 18 months from production, the physical stability of the IND loaded into the MPs was
252 assessed by FT-IR analysis and by measuring the drug content. The solid state properties of the
253 MPs were studied by means of X-ray powder diffraction analysis. Moreover, dissolution studies
254 were performed to examine possible changes in the biopharmaceutical properties of the MPs.

255

256 **Statistical Analysis**

257 One-way analysis of variance (ANOVA) followed by the Bonferroni posthoc test (GraphPadPrism,
258 GraphPad software Inc., CA, USA) was used. For the data of solubility studies the level of
259 significance was set at the probabilities of * $p < 0.05$, ** $p < 0.01$ and *** $p < 0.001$. For the data of
260 AUC values obtained by oral administrations $p < 0.001$ was considered statistically significant.

261

262

263 **3. Results and discussion**

264 **Production of IND-loaded MPs: morphology, particle size and drug loading**

265 Spray congealing (SC) technology allows the preparation of solid microparticles (MPs) by
266 solidification of the atomized molten fluid along a cooling chamber. Preliminary SC experiments
267 showed that it was not possible to obtain solid MPs using Gelucire 48/16 as the only carrier; in fact
268 after atomization, the droplets could not harden during the fall into the cooling chamber, kept at
269 room temperature. However, a binary system of Gelucire 48/16 and Gelucire 50/13 was identified
270 as suitable for SC production. Different weight ratios between the carriers were tested (**Table 1**) and
271 the formulation with the highest possible amount of Gelucire 48/16 was MPs C, containing 70%
272 w/w of Gelucire 48/16. It is also important to highlight that in the first step of the SC process, IND
273 completely solubilized in the molten Gelucire forming a bright yellow fluid. IND amount was
274 selected as 10% w/w. Considering that common dosage forms of IND are capsules containing 25 or
275 50 mg of API, our dosage form would therefore result in a capsule weighting 250-500 mg, which is
276 largely below the upper limit for the mass of a tablet or capsule (about 1 g) [4] [20]. Therefore, our
277 approach is feasible by using a drug loading of 10% for this particular API.

278 All MPs exhibited an experimental drug loading (DL) similar to the theoretical one (10% w/w),
279 hence the encapsulation efficiency (EE) was very close to 100%. Notably, excellent EE values are
280 usually obtained with SC technology [21], representing one of the major advantages of this method.

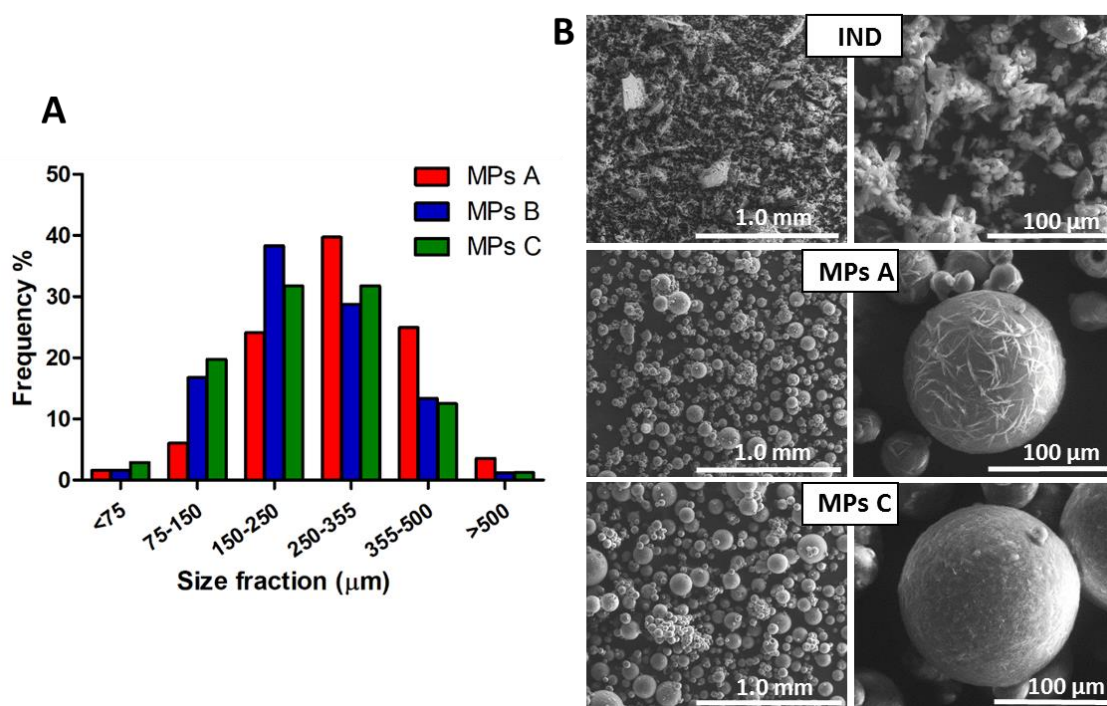
281

Sample	Costituents (% w/w)			DL (%, w/w ± SD)	EE (%)
	Gelucire 50/13	Gelucire 48/16	IND		
MPs A	90	-	10	10.73 ± 0.14	107.26 ²⁸³
MPs B	45	45	10	9.91 ± 0.22	99.06 ²⁸⁴
MPs C	27	63	10	10.06 ± 0.20	100.61 ²⁸⁵

286 **Table 1.** Composition, drug loading (DL) and encapsulation efficiency (EE) values of IND-loaded
287 MPs

288

289 **Figure 1a** shows an unimodal Gaussian particle size distribution for all formulations. More than
290 90% of MPs presented average diameter between 75 and 500 μm , with minor differences regarding
291 the prevalent size fraction, which was 250-355 μm for MPs A and 150-250 μm for MPs B and MPs
292 C. SEM images of IND and particles (MPs A and MPs C) are reported in **Figure 1b** (on the left:
293 low mag. and on the right: high mag.). SEM analysis revealed the successful formation of spherical
294 MPs; the particle surface of MPs A showed some needle-like crystals, which were absent in MPs C.



295

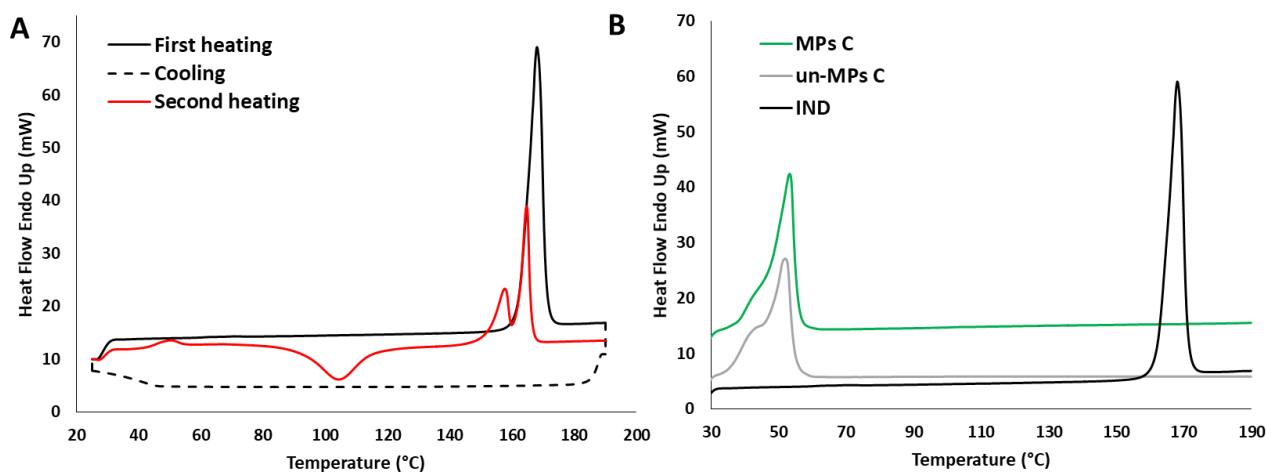
296 **Figure 1.** Particle size distribution of MPs A, MPs B and MPs C (A), SEM images of pure IND,
297 MPs A and MPs C after preparation (B).

298

299 Solid state characterization of IND-loaded MPs

300 IND is known to have a complex solid phase behaviour which include an amorphous form and at
301 least 4 polymorphic forms [22]. Notably, the fact that IND solubilized in melted Gelucire might

302 indicate the formation of MPs as solid solutions, with the drug molecularly dispersed into the
303 carrier. Otherwise, the drug might have undergone re-crystallization during the solidification step,
304 leading to the formation of solid dispersions. To have a clear and precise vision of the
305 physicochemical properties of the loaded drug and understand their influence on the
306 biopharmaceutical properties of the final formulation, a detailed solid state characterization was
307 carried out. In order to gain information about the original polymorphic form of IND, a DSC cycle
308 (**Figure 2a**) was performed by a first heating step followed by a cooling step and then a second
309 heating step. In the first step of the cycle, a single sharp melting endotherm was observed at 161.2
310 °C (onset=157.5°C) with heat of fusion of 119.11 J/g. During the cooling step, no event correlated
311 to IND crystallization was detected, suggesting the conversion in the amorphous form. Indeed, in
312 the following re-heating step the amorphous IND exhibited a T_g at 40.7 °C followed by
313 recrystallization at 101.6 °C (onset temperature and ΔH were 89.1 °C and -66.23J/g, respectively).
314 In addition, two melting endothermic peaks were observed at 151.8°C (onset=147.4°C) and 158.5
315 °C (onset=156.2°C). Those results were in accordance with the literature [22] [23] and revealed that
316 original IND was the stable γ -form. **Figure 2b** shows the DSC results of the unloaded and IND-
317 loaded MPs C. The thermogram of *un*-MPs C displayed a broad endothermic event characterized by
318 a small pre-transition and a main transition at 45.9 °C (onset=40.8°C), indicating the melting of the
319 carrier. The DSC profile of the particles containing 10% of IND (MPs C) is very similar to the
320 unloaded one, with a broad endothermic peak corresponding to the carrier melting, showing that the
321 presence of IND had no effect on the carrier melting temperature and suggesting the crystallization
322 of Gelucire during MPs solidification in the original crystalline form. Nevertheless, in the DSC
323 curve of MPs C the melting peak of the drug was absent, and the same behaviour was noted for
324 formulations A and B (data not shown). The disappearance of the IND melting peak suggests the
325 conversion of the drug in the amorphous form after the spray congealing process. However, also the
326 dissolution of the drug crystals into the molten carrier during the DSC analysis may cause the
327 melting peak disappearance, as already noticed in the case of Gelucire 50/13 as carrier [24] [25].

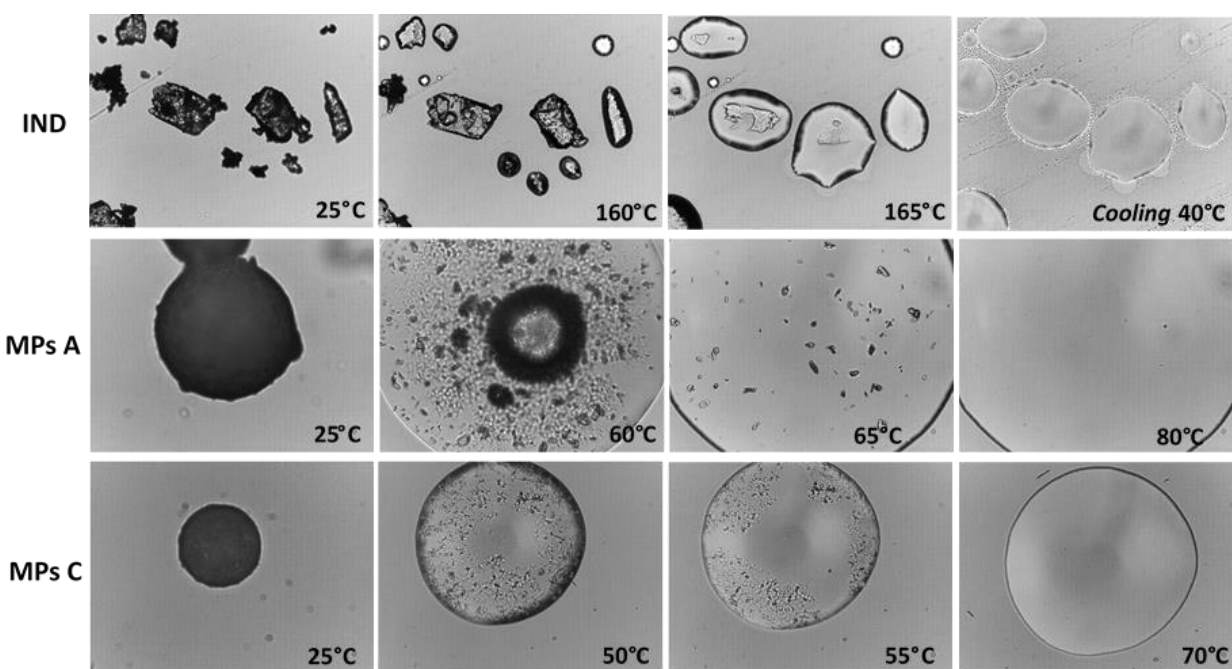


328

329 **Figure 2.** DSC cycle of IND (A) and DSC profiles of MPs C, unloaded MPs C (un-MPs C) and
 330 original IND (B).

331

332 HSM study was then performed on original drug, MPs A and MPs C (**Figure 3**) to get more
 333 information on the solid state and physicochemical properties of the drug-loaded MPs. The study
 334 confirmed the melting of IND between 160 and 165 °C. Afterwards, the sample was cooled to
 335 25°C, and interestingly the solidification occurred without evident recrystallization of the drug. In
 336 the case of MPs A, the particle started to melt at 60°C and the melting was complete at 65°C, in
 337 agreement with the melting point of Gelucire 50/13. Although small crystals were observed
 338 immediately after carrier melting, they completely disappeared as soon as the temperature was
 339 above 80°C. Differently, MPs C melted at a lower temperature (from 50 to 55°C) and no crystal
 340 was observed thereafter. The results suggested the absence of IND crystals into the MPs, and thus
 341 the presence of molecularly dispersed or amorphous IND was hypothesized. However, as also
 342 noticed in the DSC study, another possible explanation consists in the progressive melting of IND
 343 in the molten Gelucire during analysis, and the consequent lack of clearly visible crystals.

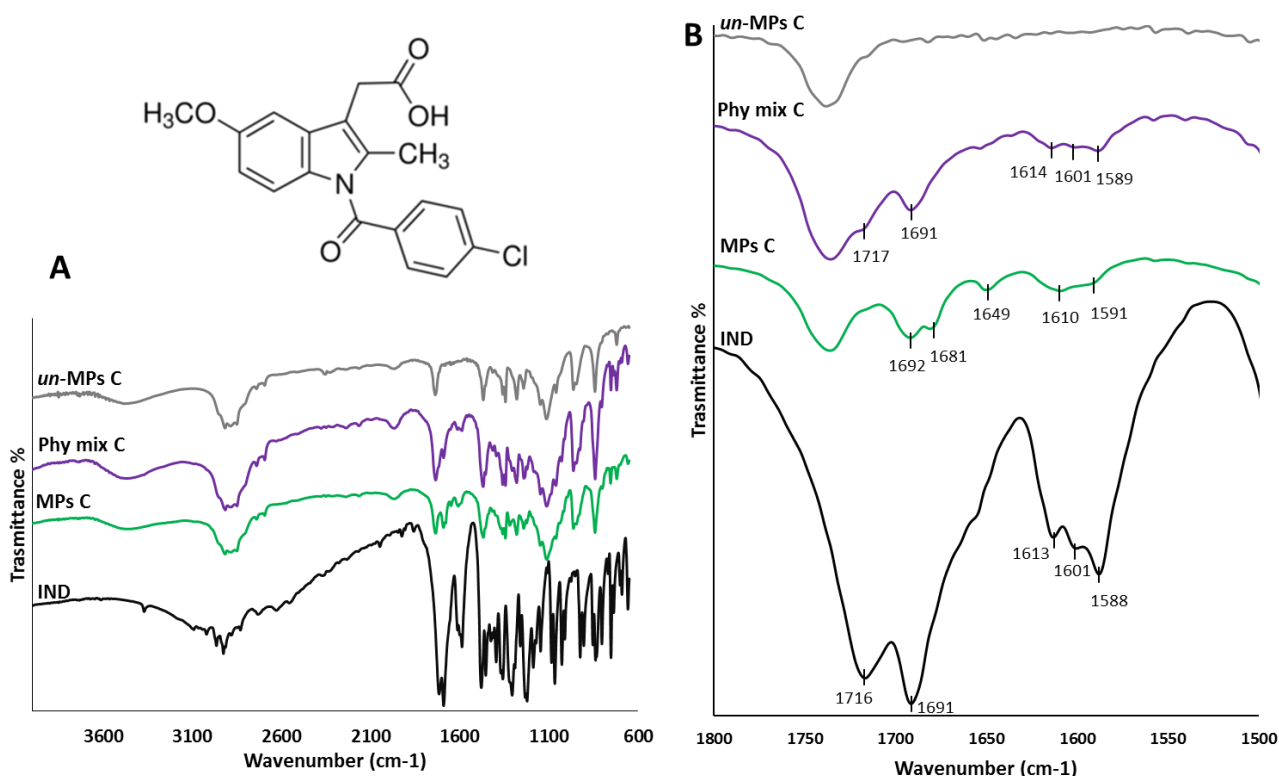


344

345 **Figure 3.** HSM images of pure IND, MPs A and MPs C during heating. For all images the
 346 magnification was set at 20x.

347 FT-IR analysis was performed to investigate the possible interactions between drug and carrier as
 348 well as to gain other information regarding IND physical state inside the MPs. **Figure 4a** reported,
 349 as example, the spectra of MPs C, Phy mix C, *un*-MP C and pure drug. IND spectrum showed sharp
 350 bands at 1716.3, 1691.3, 1613.2, 1588.1 and 1599.6 cm^{-1} , characteristics of the γ form [22] [26],
 351 confirming that the raw drug was in the stable polymorphic form. Unloaded particles showed bands
 352 typical of Gelucire: 3100-3600 cm^{-1} (broad, stretching of free OH groups), 1738.5 cm^{-1} (stretching
 353 C=O group), 1469.5 cm^{-1} (C-H deformation of alkyl group), 1113.7 cm^{-1} (-C-O stretching), and
 354 963.3 cm^{-1} (double band, characteristic of the polyethylene glycol groups) [24] [27] [28]. MPs and
 355 Phy mix present FT-IR spectra similar to the unloaded particles but with some extra band that can
 356 be ascribed to the presence of drug, although with lower intensity due to the limited content of drug
 357 in the sample (10%). To allow a better analysis of the results, the spectra of MPs and Phy mix were
 358 compared in the region between the wavenumbers 1800-1500 cm^{-1} , specific for the carbonyl
 359 stretching. As visible in **Figure 4b**, the carrier presents only one band at 1720-1750 cm^{-1} with no
 360 other bands in this region, thus the extra bands present in Phy mix and MPs samples can be ascribed
 361 to IND. Interestingly, various differences were detected between the two samples. Notably, the

362 specific bands positions of IND in the Phy mix C corresponded to the original IND crystalline form
363 γ , and the same bands were observed for Phy mix A and B (data not shown). The bands of IND
364 were observed at different wavenumbers in case of all MPs formulations (**Figure 4b** for MPs C,
365 data not shown for MPs A and MPs B). The differences in the carbonyl stretching region depend on
366 the hydrogen-bonding of the carboxylic acid and amide carbonyl group of IND, which can have
367 different arrangements in the various drug solid forms [29]. The bands detected in the MPs in this
368 region (at wavenumbers of 1681, 1591 and 1610 cm^{-1}) were similar to the characteristic signals of
369 the amorphous form, whereas the band at 1649 cm^{-1} is characteristic α -form [30]. Additionally, the
370 strong band (at 1734 cm^{-1} and 1735 cm^{-1} for α and amorphous forms, respectively) assigned to the
371 non-hydrogen bonded carboxylic acid was missing. Therefore, these data provided a clear
372 indication that spray congealing process modified the IND solid state, but further analysis were
373 needed to confirm the solid state form of IND in our system.

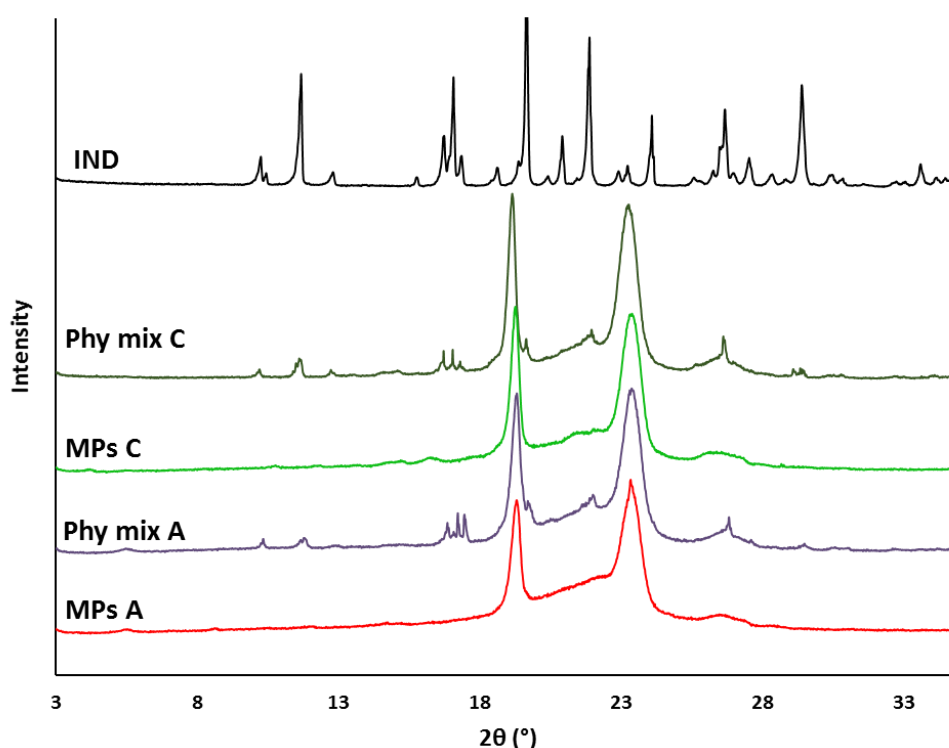


374

375 **Figure 4.** FT-IR spectra of IND, MPs C, Phy mix C and *un*-MPs C in the spectral region between
376 4000 and 400 cm^{-1} (A) and focus on the carbonyl stretching region 1800-1500 cm^{-1} (B).

377 PXRD analysis were thus performed; the results are shown in **Figure 5**. The diffractogram of IND
378 showed main peaks at 11.6, 17.1, 19.7, 21.9, 26.7 and 29.4 of 2θ , confirming that the raw drug was
379 in the crystalline γ form. The XRD spectra of both formulations A and C physical mixtures showed,
380 besides the two main peaks at 19.3 and 23.5 of 2θ typical of Gelucires [16] [25], all the
381 characteristics peaks of γ IND, although less intense due to the small amount (10% w/w) of the
382 drug. On the contrary, the diffractograms of either MPs A and MPs C showed only the peaks
383 correspondent to the carrier, and no distinct peak attributable to IND was detected. These results
384 indicated a loss of IND crystallinity into the spray-congealed MPs.

385



386

387 **Figure 5.** Powder X-Ray diffractograms of raw IND, IND-loaded MPs and the correspondent
388 physical mixture (formulations A and C).

389

390 Gelucire 50/13 has been used as carrier for different poorly water soluble APIs with formation of
391 either *solid solutions* of the drug molecularly dispersed within the carrier, as in the case of ursolic
392 acid [16] or *solid dispersions* with crystalline drug molecules, such as for piroxicam [31],

393 carbamazepine [24] and praziquantel [25]. The formation of one of the other system depends on the
394 solubility of the drug into the Gelucire at the molten state. In the present study, the solid state
395 characterization data suggested the presence of non-crystalline IND in crystalline carrier Gelucire.
396 IND-loaded MPs could be thus considered a solid solution, defined as a system in which one solid
397 component is (at least partially) dissolved in the other solid component, resulting in a one-phase
398 system [4]. On the other hand, the experimental results do not exclude that API molecules may exist
399 as separated amorphous phase or may be present in an intimate mixture with the crystalline carrier
400 in which the degree of contact may vary from fully miscible (solid solution) to partly separated
401 domains of the drug [32].

402

403 ***In vitro* dissolution and solubility studies**

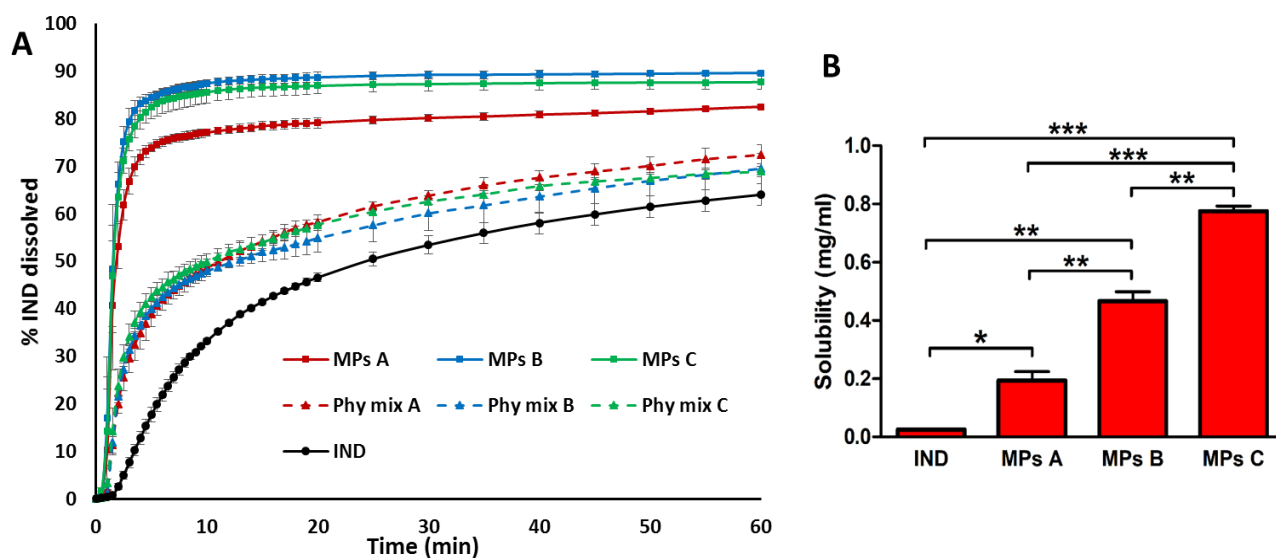
404 IND (pKa 4.5) can be considered practically insoluble in simulated gastric fluid (pH 1.2) and
405 slightly soluble in simulated intestinal fluid (pH 7.4) [33]. Since IND solubility increases with the
406 raising of the pH, the drug absorption is facilitated in intestinal environment, where the pH is higher
407 compared to the gastric fluid. However, intestinal pH values weakly acidic are not uncommon,
408 especially in fed conditions, where the average pH is reported to be around 5.8 [34], thus leading to
409 a difficult drug dissolution. For this reason, in the present research the dissolution and solubility
410 studies were performed in weakly acidic buffer (pH 5.8) rather than at neutral pH (i.e. pH 6.8 or
411 7.4), in order to simulate the least favourable (and more challenging) intestinal condition.

412 *In vitro* dissolution profiles are reported in **Figure 6a**. Dissolution profiles were compared using the
413 “similarity factor, f_2 ”. IND powder showed the slowest dissolution rate, with 53% of drug dissolved
414 within 30 min. Phy mix A, B and C improved IND dissolution rate ($f_2 = 39.3, 39.2$ and 36.3 for Phy
415 mix A, B and C respect to IND, respectively), with an effect more evident in the beginning of the
416 test, probably attributed to the improvement of wettability [35]. MPs A considerably enhanced IND
417 dissolution rate, leading to 80 % of drug dissolution within 30 minutes. The highest dissolution rate

418 was achieved by MPs B and MPs C, with 89 and 87% of drug dissolved in the first 30 min,
419 respectively. Specifically, the dissolution performance of MPs resulted different from both the
420 correspondent physical mixtures ($f_2= 26.7, 20.3$ and 22.7 for formulation A, B and C, respectively)
421 and IND with f_2 values lower than 20 ($f_2= 17.1, 12.8$ and 13.6 for MPs A, B and C, respectively).
422 The dissolution profiles of the different MPs formulations resulted not significantly different ($f_2 \geq$
423 50) indicating no substantial influence of the Gelucire 50/13 and 48/16 ratio on IND dissolution
424 profiles. Overall, the significantly different dissolution profiles given by the physical mixtures
425 compared to those given by the MPs could be correlated to different mechanisms. In the case of
426 physical mixtures, the improvement of wettability of IND and the solubilisation of the drug by
427 Gelucire at the diffusion layer [36] are likely to be the main mechanisms involved. Moreover, the
428 surface active properties of Gelucire may influence both drug dissolution rate and solubility by
429 formation of micelles. In the case of spray congealed-MPs, we suppose that additional mechanisms
430 are involved. The presence of the drug embedded in the hydrophilic excipient can further improve
431 the wetting and dissolution. Qi et al. suggested that, during dissolution, this excipient is subjected to
432 swelling (hydration) and formation of a liquid crystalline phase. This process can facilitate the
433 wetting of the drug particles embedded in the microspheres and maximise the surface area via
434 prevention of aggregation [31]. In addition, the loss of crystallinity of IND in Gelucire-based
435 system, as demonstrated by solid state results, surely represents an advantage in terms of dissolution
436 rate. It is well known that the absence of drug crystals improve dissolution rate as the energy
437 normally required to break up the ordered crystalline structure is no longer a limitation.

438 In addition to the dissolution rate, the change in IND solid state as well as the formation of micelles
439 can both determine an enhancement in drug solubility, which was evaluated in phosphate buffer
440 (pH 5.8). As expected, the solubility of IND from MPs A, MPs B and MPs C (**Figure 6b**) was
441 $0.194 \pm 0.044, 0.466 \pm 0.045$ and 0.775 ± 0.025 mg/mL, respectively. Compared to free IND (0.025
442 ± 0.002 mg/mL), the solubility of IND formulated into MPs A, B and C was approximately 4-, 19-,
443 and 31-fold higher, respectively. Specifically, the enhancement of solubility with increasing amount

444 of Gelucire 48/16 in the formulation indicates a better solubilisation ability of this excipient. MPs C
445 were therefore selected for oral administration studies.



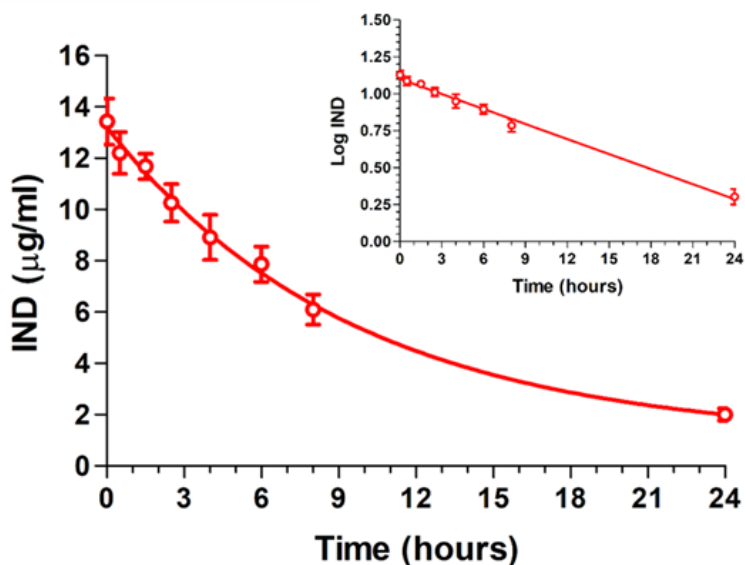
446

447 **Figure 6.** (a) Dissolution profiles of IND, MPs and physical mixtures (Phy mix) in phosphate buffer
448 pH 5.8 and (b) 48 h equilibrium solubility of IND and MPs in phosphate buffer pH 5.8. Data
449 represent mean \pm S.D. ($n = 3$), and the level of significance was set at the probabilities of $*p < 0.05$,
450 $**p < 0.01$, and $***p < 0.001$.

451

452 *In vivo* bioavailability studies

453 After intravenous (IV) infusion of 0.90 mg IND, the drug concentration in the rat bloodstream was
454 $13.43 \pm 0.9 \mu\text{g/mL}$. This value decreased during time with an apparent first order kinetic (Figure 7)
455 confirmed by the linearity of the semilogarithmic plot reported in the inset of Figure 7 ($n = 8$, $r =$
456 0.996 , $P < 0.0001$), showing an half-life value of 8.84 ± 0.31 hours. These data are in good
457 agreement with those obtained by previous studies on IND pharmacokinetics [37].



458

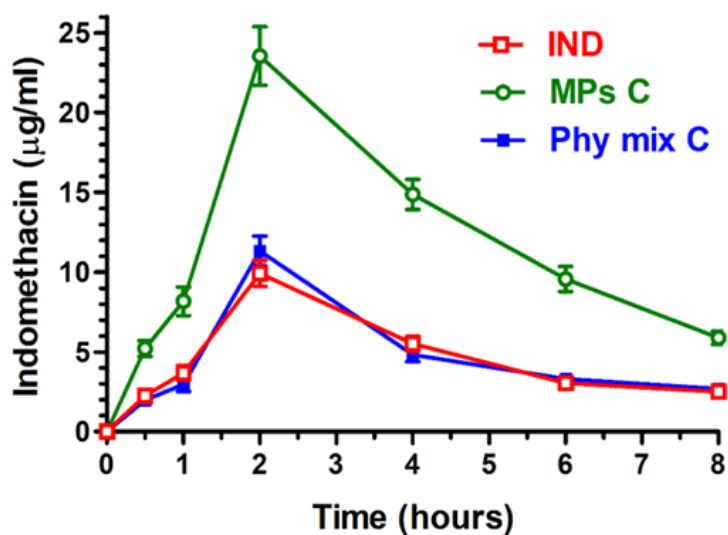
459 **Figure 7.** Elimination profile of indomethacin after 0.90 mg IV infusion to rats. The elimination
 460 followed an apparent first order kinetic, confirmed by the semilogarithmic plot reported in the inset
 461 ($n = 8$, $r = 0.996$, $P < 0.0001$). The half-life of IND was calculated to be 8.84 ± 0.31 hours.

462 All data are expressed as the mean \pm SD of four independent experiments.

463

464 Figure 8 reported the rat blood IND concentrations within 8 hours the oral administration of 2.0 mg
 465 of drug (about 8 mg/kg) as powders of free γ -IND, its physical mixture with unloaded MPs C (Phy
 466 mix C), or IND-loaded MPs C (MPs C). It can be observed that the free γ -IND powder induced a
 467 concentration peak in the rat bloodstream of about 10 $\mu\text{g/mL}$ two hours after the administration
 468 (T_{max}) and a similar profile was obtained with the Phy mix C. These data appear in agreement with
 469 those obtained by previous studies, indicating IND peak concentrations in bloodstream of rats of
 470 around 30 $\mu\text{g/mL}$ two hours after the administration of 22.5 mg/kg of IND suspended in methyl
 471 cellulose [38]. In addition, it is reported that the oral administration of 0.9 mg IND (about 3.6
 472 mg/kg) as solid powder to rats induces peak concentrations in the bloodstream near to 5 $\mu\text{g/mL}$,
 473 with a corresponding T_{max} value of two hours [37].

474 On the other hand, the profile resulting from loaded MPs C showed a peak concentration of about
 475 24 $\mu\text{g/mL}$ two hours after its administration (Figure 8).



476

477 **Figure 8.** Blood IND concentrations ($\mu\text{g/mL}$) obtained by oral administration of 2.0 mg dose to rats
 478 within 8 hours. The formulations were constituted by the powders of free γ -indomethacin (IND), its
 479 physical mixture with unloaded MPs C (Phy mix C), or IND-loaded MPs C (MPs C). All data are
 480 expressed as the mean \pm SD of four independent experiments.

481

482 As reported in Table 2, it can be observed that the AUC value obtained by the oral administration of
 483 free γ -IND ($70.55 \pm 2.26 \mu\text{g}\cdot\text{mL}^{-1}\cdot\text{h}$) was not significantly different ($P > 0.05$) from the AUC value
 484 obtained by the physical mixture administration ($76.99 \pm 2.26 \mu\text{g}\cdot\text{mL}^{-1}\cdot\text{h}$), whereas a significant
 485 difference ($P < 0.001$) was detected between the AUC values obtained by the oral administration of
 486 free γ -IND and MPs C.

487

488

489

Formulation	IND dose	AUC ($\mu\text{g}\cdot\text{mL}^{-1}\cdot\text{h}$)	Absolute Bioavailability (F)
IND (IV)	0.9 mg	165.06 ± 6.2	--
IND (oral)	2.0 mg	70.55 ± 2.26	19.20%
Phy mix C	2.0 mg	$76.99 \pm 2.26^*$	20.98 %
MPs C	2.0 mg	$174.3 \pm 5.8^{**}$	47.51%

490

491 **Table 2.** AUC values obtained by intravenous (IV) infusion of 0.9 mg indomethacin (IND IV) or by
492 the oral administration of 2 mg of indomethacin (IND oral), its physical mixture with unloaded MPs
493 C (Phy Mix C), or encapsulated in MPs C (MPs C). All the AUC values are reported as the mean \pm
494 SD of four independent experiments. The absolute bioavailability values were calculated by the
495 AUC data normalized with respect to their IND doses. * $p > 0.05$ versus IND (oral); ** $p < 0.001$
496 versus IND (oral).

497

498 In particular, the AUC value of the microparticulate formulation was $174.3 \pm 5.8 \mu\text{g}\cdot\text{mL}^{-1}\cdot\text{h}$, about
499 2.5 times higher than the AUC value of free γ -IND. These data indicate that the formulation of IND
500 into Gelucire-based MPs allows to sensibly increase the amounts of IND absorbed in the
501 bloodstream. Interestingly, no significant effect was observed on the absorption rate of IND in the
502 bloodstream, being 2 h the T_{max} values for all the samples tested. A similar behaviour was
503 previously registered with IND formulations constituted by self-emulsifying systems [38].

504 The ability of the MPs C to increase *in vivo* IND bioavailability was therefore attributable to the
505 microparticulate formulation and not to its excipients, being the AUC value of the physical mixture
506 not significantly different to that of free γ -IND. Although the physical mixtures led to a small
507 enhancement of IND *in vitro* dissolution rate (Figure 6), the improvement of the drug wettability
508 promoted by the presence of Gelucire did not induce a significant effect on the drug absorption in
509 the bloodstream. This can be explained by considering that the effect of increased wettability might
510 be induced either way by other components of the GIT, such as bile acid salts, released by the gall
511 bladder for the emulsification of hydrophobic compounds during digestion [39].

512 The AUC values of the profiles reported in Figures 7 and 8 were used for the calculation of absolute
513 bioavailability (F) values of the solid formulations, which are reported in Table 2. The F values
514 were calculated by the AUC data normalized with respect to their IND doses. In this case the IND
515 dose for the IV administration was 0.9 mg for each rat (about 3.6 mg/Kg), being the maximum
516 amount allowing to obtain solubilized IND in 1 mL of the medium constituted by 20% (v/v) DMSO

517 and 80% (v/v) physiologic solution. The IND dose for the oral administration was 2 mg for each rat
518 (about 8 mg/kg), a value included between 1.85 mg/kg and 22.5 mg/kg, a range normally used for
519 oral bioavailability studies of this drug [19] [37] [38] [40].

520 The F values of γ -IND in the free form, or mixed with unloaded MPs C, were about the 20%, in
521 accordance with previous studies [37]. According to these studies, we evidenced that an approach of
522 co-crystallization of IND can induced the increase of both water solubility and oral bioavailability
523 of this drug. As an example, the co-crystallization of IND with saccharin or 2-hydroxy-4-methyl-
524 pyridine induced a drug bioavailability increase from the 23% to the 34% or 38%, respectively [37].
525 Unfortunately, 2-hydroxy-4-methyl-pyridine is characterized by acute toxicity for our body.
526 According to the measurements here reported, the oral administration of the loaded MPs C allowed
527 to obtain a F value of 47.51%, about 2.5 times higher than that obtained with the free γ -IND,
528 indicating the ability of the MPs to sensibly increase the oral IND bioavailability. It is important to
529 remark that this bioavailability enhancement was obtained with a formulation characterized by high
530 biocompatibility, being Gelucire recognized as Safe (GRAS) and oral-approved.

531

532 **Stability studies**

533 No statistical change in drug content was found for all samples ($p > 0.05$) after 18 months of storage
534 (data not shown), indicating that all the formulations were physically stable with no loss or
535 degradation of the drug during storage. Moreover, the FT-IR analysis of MPs C (Figure 1 of the
536 supplementary material) showed all the characteristic peaks correspondent to IND and excipient
537 kept unchanged, suggesting the absence of interaction between carrier and drugs during long-term
538 storage. IND solid state in MPs A and MPs C after 18 months was characterized by XRPD. As
539 shown in Figure 2 SI, the diffractograms showed no evident change in the pattern compared to the
540 zero time samples, therefore suggesting the stability of the IND amorphous form. Additionally, the

541 dissolution profile of the formulation C (Figure 3 SI) resulted unchanged after 18 months storage,
542 thus confirming the stability of the pharmaceutical performance of this formulation.

543 The stability of the drug in the amorphous form represent a major challenge in the development of
544 solid dispersions. A number of factors, such as molecular mobility, thermodynamic properties,
545 environmental stress, preparation methods, and storage conditions contribute to determine the
546 stability of the drug amorphous form [41]. Changings in polymorphic form of IND in dispersion
547 with hydrophilic carrier have been previously reported. Recently, Van Duong et al. reported the
548 study of semicrystalline dispersions of IND in PEG where the crystallization of the drug was
549 observed at different times, depending on the drug loading [29]. The SD with 10% of IND, the same
550 drug loading of our system, showed the longest time for IND recrystallization compared to the SD
551 with higher drug loadings. In our study, the SD **showed no trace of recrystallization** for at least 18
552 months. In case of low drug loadings, the amount of drug is generally insufficient to affect the
553 carrier crystallization during solidification from the melt [29] [42]. Thus, during solidification of the
554 MPs, the dispersions exhibits instant crystallization of Gelucire (Figure 2b) with **amorphous or**
555 **molecularly dispersed drug** entrapped in the ordered crystalline matrix (Figure 5). The mobility of
556 IND molecules would be thus extremely low in the highly viscous crystalline Gelucire matrix.
557 Therefore, we hypothesize that the crystallization of IND in the SD was prevented because of the
558 lack of molecular mobility required for nucleation and crystal growth.

559

560 **4. Conclusions**

561 In this work, spray congealing technology has been explored to produce solid dispersion with
562 enhanced oral indomethacin bioavailability. Spray congealing enabled the preparation of MPs with
563 encapsulation efficiency values closer to 100%. The MPs were spherical and free flowing, thus
564 ready-to-use for tableting or capsule filling. The new excipient Gelucire 48/16 showed great
565 potential for the bioavailability enhancement of IND. Specifically, the formulation with 30%

566 Gelucire 50/13 and 70% Gelucire 48/16 (MPs C) led to an important increase in drug solubility and
567 a considerable enhancement of drug dissolution rate compared with the pure drug. *In vivo*
568 pharmacokinetic studies indicate that MPs C allows to significantly increase (about 2.5 times) the
569 oral bioavailability of the drug. The bioavailability enhancement was mainly due to the conversion
570 of IND into the amorphous form, as confirmed by solid state characterization, which was
571 maintained during storage.

572 Overall, the low-cost and easily scaled-up spray congealing technology allowed to produce MPs
573 with consistent and reproducible *in vitro* and *in vivo* performances as well as ideal technological
574 properties. Thus, spray congealing is a promising approach for the industrial production of stable
575 SD with amorphous IND dispersed in crystalline Gelucire.

576

577 **Acknowledgements**

578 This research did not receive any specific grant from funding agencies in the public, commercial, or
579 not-for-profit sectors.

580

581

582

583 **References**

- 584 [1] J.L. Ford, M.H. Rubinstein, Phase equilibria and dissolution rates of indomethacin-
585 polyethylene glycol 6000 solid dispersions, *Pharm. Acta Helv.* 53 (1978) 327—332.
- 586 [2] D.N. Bikiaris, Solid dispersions, Part II: new strategies in manufacturing methods for
587 dissolution rate enhancement of poorly water-soluble drugs, *Expert Opin. Drug Deliv.* 8
588 (2011) 1663–1680. doi:10.1517/17425247.2011.618182.

- 589 [3] J. Guan, Q. Liu, X. Zhang, Y. Zhang, R. Chokshi, H. Wu, S. Mao, Alginate as a potential
590 diphasic solid dispersion carrier with enhanced drug dissolution and improved storage
591 stability, *Eur. J. Pharm. Sci.* 114 (2018) 346–355. doi:10.1016/j.ejps.2017.12.028.
- 592 [4] C. Leuner, J. Dressman, Improving drug solubility for oral delivery using solid dispersions,
593 *Eur. J. Pharm. Biopharm.* 50 (2000) 47–60.
- 594 [5] S. Huang, R.O. Williams, Effects of the preparation process on the properties of amorphous
595 solid dispersions, *AAPS PharmSciTech.* 19 (2017) 1971–1984. doi:10.1208/s12249-017-
596 0861-7.
- 597 [6] X. Liu, X. Feng, R.O. Williams, F. Zhang, Characterization of amorphous solid dispersions,
598 *J. Pharm. Investig.* 48 (2018) 19–41. doi:10.1007/s40005-017-0361-5.
- 599 [7] S. Dedroog, C. Huygens, G. Van Den Mooter, Chemically identical but physically different :
600 A comparison of spray drying , hot melt extrusion and cryo-milling for the formulation of
601 high drug loaded amorphous solid dispersions of naproxen, *Eur. J. Pharm. Biopharm.* 135
602 (2019) 1-12. doi:10.1016/j.ejpb.2018.12.002.
- 603 [8] S. Nalamachu, R. Wortmann, Role of Indomethacin in acute pain and inflammation
604 management: A review of the literature, *Postgrad. Med.* 126 (2014) 92–97.
605 doi:10.3810/pgm.2014.07.2787.
- 606 [9] A. Dalmoro, S. Bochicchio, S.F. Nasibullin, P. Bertocin, G. Lamberti, A. Angela, R.I.
607 Moustafa, Polymer-lipid hybrid nanoparticles as enhanced indomethacin delivery systems, *Eur.*
608 *J. Pharm. Sci.* 121 (2018) 16–28. doi:10.1016/j.ejps.2018.05.014.
- 609 [10] C. Aloisio, A. G. de Oliveira, M. Longhi, Cyclodextrin and Meglumine-based
610 microemulsions as a poorly water-soluble drug delivery system, *J. Pharm. Sci.* 105 (2016)
611 2703–2711. doi:https://doi.org/10.1016/j.xphs.2015.11.045.
- 612 [11] M.M. Mehanna, J.K. Alwattar, H.A. Elmaradny, Optimization, physicochemical

- 613 characterization and in vivo assessment of spray dried emulsion: A step toward
614 bioavailability augmentation and gastric toxicity minimization, *Int. J. Pharm.* 496 (2015)
615 766–779. doi:10.1016/j.ijpharm.2015.11.009.
- 616 [12] V.P. Sant, D. Smith, J.-C. Leroux, Novel pH-sensitive supramolecular assemblies for oral
617 delivery of poorly water soluble drugs: Preparation and characterization, *J. Control. Release.*
618 97 (2004) 301–312. doi:10.1016/j.jconrel.2004.03.026.
- 619 [13] S. Bertoni, L.S. Dolci, B. Albertini, N. Passerini, Spray congealing: a versatile technology
620 for advanced drug delivery systems, *Ther. Deliv.* 9 (2018) 833–845.
- 621 [14] N. Chella, R. Tadikonda, Melt dispersion granules: formulation and evaluation to improve
622 oral delivery of poorly soluble drugs – a case study with valsartan, *Drug Dev. Ind. Pharm.* 41
623 (2015) 888–897. doi:10.3109/03639045.2014.911308.
- 624 [15] S. Jammula, C.N. Patra, S. Swain, K.C. Panigrahi, S. Nayak, S.C. Dinda, M.E.B. Rao,
625 Design and characterization of cefuroxime axetil biphasic floating minitablets, *Drug Deliv.*
626 22 (2015) 125–135. doi:10.3109/10717544.2013.871603.
- 627 [16] J. de Oliveira Eloy, J. Saraiva, S. de Albuquerque, J.M. Marchetti, Solid dispersion of ursolic
628 acid in Gelucire 50/13: a strategy to enhance drug release and trypanocidal activity., *AAPS*
629 *PharmSciTech.* 13 (2012) 1436–45. doi:10.1208/s12249-012-9868-2.
- 630 [17] N. Passerini, B. Perissutti, B. Albertini, E. Franceschinis, D. Lenaz, D. Hasa, I. Locatelli, D.
631 Voinovich, A new approach to enhance oral bioavailability of Silybum Marianum dry
632 extract: Association of mechanochemical activation and spray congealing, *Phytomedicine.* 19
633 (2012) 160–168. doi:10.1016/j.phymed.2011.06.027.
- 634 [18] T. Van Duong, G. Van den Mooter, The role of the carrier in the formulation of
635 pharmaceutical solid dispersions. Part II: amorphous carriers, *Expert Opin. Drug Deliv.* 13
636 (2016) 1681–1694. doi:10.1080/17425247.2016.1198769.

- 637 [19] S. Simovic, P. Heard, H. Hui, Y. Song, F. Peddie, A.K. Davey, A. Lewis, T. Rades, C.A.
638 Prestidge, Dry hybrid lipid–silica microcapsules engineered from submicron lipid droplets
639 and nanoparticles as a novel delivery system for poorly soluble drugs, *Mol. Pharm.* 6 (2009)
640 861–872. doi:10.1021/mp900063t.
- 641 [20] A.H. Goldberg, M. Gibaldi, J.L. Kanig, Increasing dissolution rates and gastrointestinal
642 absorption of drugs via solid solutions and eutectic mixtures I: Theoretical considerations and
643 discussion of the literature, *J. Pharm. Sci.* 54 (1965) 1145–1148.
644 doi:<https://doi.org/10.1002/jps.2600540810>.
- 645 [21] S. Bertoni, B. Albertini, L.S. Dolci, N. Passerini, Spray congealed lipid microparticles for the
646 local delivery of β -galactosidase to the small intestine, *Eur. J. Pharm. Biopharm.* 132 (2018)
647 1–10. doi:10.1016/j.ejpb.2018.08.014.
- 648 [22] S.A. Surwase, J.P. Boetker, D. Saville, B.J. Boyd, K.C. Gordon, L. Peltonen, C.J. Strachan,
649 Indomethacin: New polymorphs of an old drug, *Mol. Pharm.* 10 (2013) 4472–4480.
650 doi:10.1021/mp400299a.
- 651 [23] N. Kaneniwa, M. Otsuka, T. Hayashi, Physicochemical characterization of Indomethacin
652 polymorphs and the transformation kinetics in ethanol, *Chem. Pharm. Bull.* 33 (1985) 3447–
653 3455.
- 654 [24] N. Passerini, B. Perissutti, M. Moneghini, D. Voinovich, B. Albertini, C. Cavallari, L.
655 Rodriguez, Characterization of Carbamazepine - Gelucire 50 / 13 microparticles prepared by
656 a spray-congealing process using ultrasounds, *J. Pharm. Sci.* 91 (2002) 699–707.
- 657 [25] N. Passerini, B. Albertini, B. Perissutti, L. Rodriguez, Evaluation of melt granulation and
658 ultrasonic spray congealing as techniques to enhance the dissolution of praziquantel, *Int. J.*
659 *Pharm.* 318 (2006) 92–102. doi:10.1016/j.ijpharm.2006.03.028.
- 660 [26] A. Fini, C. Cavallari, F. Ospitali, Raman and thermal analysis of indomethacin / PVP solid

- 661 dispersion enteric microparticles, *Eur. J. Pharm. Biopharm.* 70 (2008) 409–420.
662 doi:10.1016/j.ejpb.2008.03.016.
- 663 [27] R.M. Martins, S. Siqueira, M.O. Machado, R. Molina, S. Siqueira, M.O. Machado, R.M.
664 Martins, S. Siqueira, M.O. Machado, L. Alexandre, P. Freitas, The effect of homogenization
665 method on the properties of carbamazepine microparticles prepared by spray congealing
666 carbamazepine microparticles prepared by spray congealing, *J Microencapsul.* 30 (2013)
667 692–700. doi:10.3109/02652048.2013.778906.
- 668 [28] M. El Hadri, A. Achahbar, J. El Khamkhami, B. Khelifa, V. Faivre, O. Abbas, S. Bresson,
669 Lyotropic behavior of Gelucire 50/13 by XRD, Raman and IR spectroscopies according to
670 hydration, *Chem. Phys. Lipids.* 200 (2016) 11–23. doi:10.1016/j.chemphyslip.2016.05.005.
- 671 [29] T. Van Duong, D. Ludeker, P.-J. Van Bockstal, T. De Beer, J. Van Humbeeck, G. Van Den
672 Mooter, Polymorphism of Indomethacin in semicrystalline dispersions: formation,
673 transformation, and segregation, *Mol. Pharm.* 15 (2018) 1037–1051.
674 doi:10.1021/acs.molpharmaceut.7b00930.
- 675 [30] C.J. Strachan, T. Rades, K.C. Gordon, A theoretical and spectroscopic study of γ -crystalline
676 and amorphous indometacin, *J. Pharm. Pharmacol.* 59 (2007) 261–269.
677 doi:10.1211/jpp.59.2.0012.
- 678 [31] S. Qi, D. Marchaud, D.Q.. Craig, An Investigation into the mechanism of dissolution rate
679 enhancement of poorly water-soluble drugs from spray chilled Gelucire 50/13 microspheres,
680 *J. Pharm. Sci.* 99 (2010) 262–274.
- 681 [32] O. Policianova, J. Brus, M. Hruby, M. Urbanova, A. Zhigunov, J. Kredatusova, L. Kobera,
682 Structural diversity of solid dispersions of acetylsalicylic acid as seen by solid-state NMR,
683 *Mol. Pharm.* 11 (2014) 516–530. doi:10.1021/mp400495h.
- 684 [33] K.A. Elkhodairy, N.S. Barakat, G. El-Shazli, Effect of type and concentration of release-

- 685 retarding vehicles on the dissolution rate of diltiazem hydrochloride from liquisolid compact,
686 *J. Drug Deliv. Sci. Technol.* 22 (2012) 189–195. doi:[https://doi.org/10.1016/S1773-](https://doi.org/10.1016/S1773-2247(12)50025-0)
687 2247(12)50025-0.
- 688 [34] E. Jantratid, N. Janssen, C. Reppas, J.B. Dressman, Dissolution media simulating conditions
689 in the proximal human gastrointestinal tract: An update, *Pharm. Res.* 25 (2008) 1663–1676.
690 doi:10.1007/s11095-008-9569-4.
- 691 [35] N. Ahuja, O.P. Katare, B. Singh, Studies on dissolution enhancement and mathematical
692 modeling of drug release of a poorly water-soluble drug using water-soluble carriers, *Eur. J.*
693 *Pharm. Biopharm.* 65 (2007) 26–38. doi:<https://doi.org/10.1016/j.ejpb.2006.07.007>.
- 694 [36] D.D. Sun, P.I. Lee, Probing the mechanisms of drug release from amorphous solid
695 dispersions in medium-soluble and medium-insoluble carriers, *J. Control. Release.* 211
696 (2015) 85–93. doi:<https://doi.org/10.1016/j.jconrel.2015.06.004>.
- 697 [37] V. Ferretti, A. Dalpiaz, V. Bertolasi, L. Ferraro, S. Beggiato, F. Spizzo, E. Spisni, B. Pavan,
698 Indomethacin co-crystals and their parent mixtures: Does the intestinal barrier recognize
699 them differently?, *Mol. Pharm.* 12 (2015) 1501–1511. doi:10.1021/mp500826y.
- 700 [38] J.Y. Kim, Y.S. Ku, Enhanced absorption of indomethacin after oral or rectal administration
701 of a self-emulsifying system containing indomethacin to rats, *Int. J. Pharm.* 194 (2000) 81–
702 89. doi:[https://doi.org/10.1016/S0378-5173\(99\)00367-1](https://doi.org/10.1016/S0378-5173(99)00367-1).
- 703 [39] E. Acosta, Bioavailability of nanoparticles in nutrient and nutraceutical delivery, *Curr. Opin.*
704 *Colloid Interface Sci.* 14 (2009) 3–15. doi:10.1016/j.cocis.2008.01.002.
- 705 [40] M.-S. Jung, J.-S. Kim, M.-S. Kim, A. Alhalaweh, W. Cho, S.-J. Hwang, S.P. Velaga,
706 Bioavailability of indomethacin-saccharin cocrystals, *J. Pharm. Pharmacol.* 62 (2010) 1560–
707 1568. doi:10.1111/j.2042-7158.2010.01189.x.
- 708 [41] S. Baghel, H. Cathcart, N.J.O. Reilly, Polymeric amorphous solid dispersions : A review of

709 amorphization , crystallization , stabilization , solid-state characterization , and aqueous
710 solubilization of biopharmaceutical classification system class II drugs, *J. Pharm. Sci.* 105
711 (2016) 2527–2544. doi:10.1016/j.xphs.2015.10.008.

712 [42] T. Van Duong, G. Reekmans, A. Venkatesham, A. Van Aerschot, P. Adriaensens, J. Van
713 Humbeeck, G. Van Den Mooter, Spectroscopic investigation of the formation and disruption
714 of hydrogen bonds in pharmaceutical semicrystalline dispersions, *Mol. Pharm.* 14 (2017)
715 1726–1741. doi:10.1021/acs.molpharmaceut.6b01172.

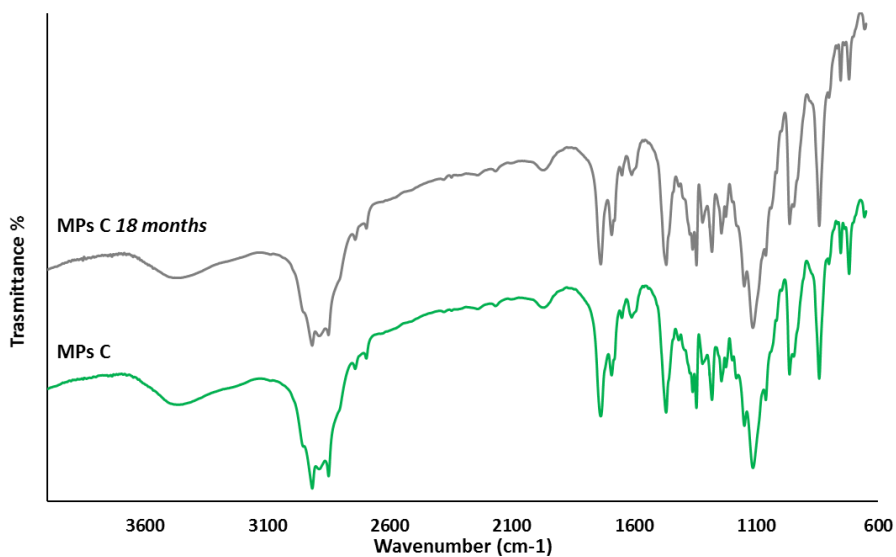
716

717

718

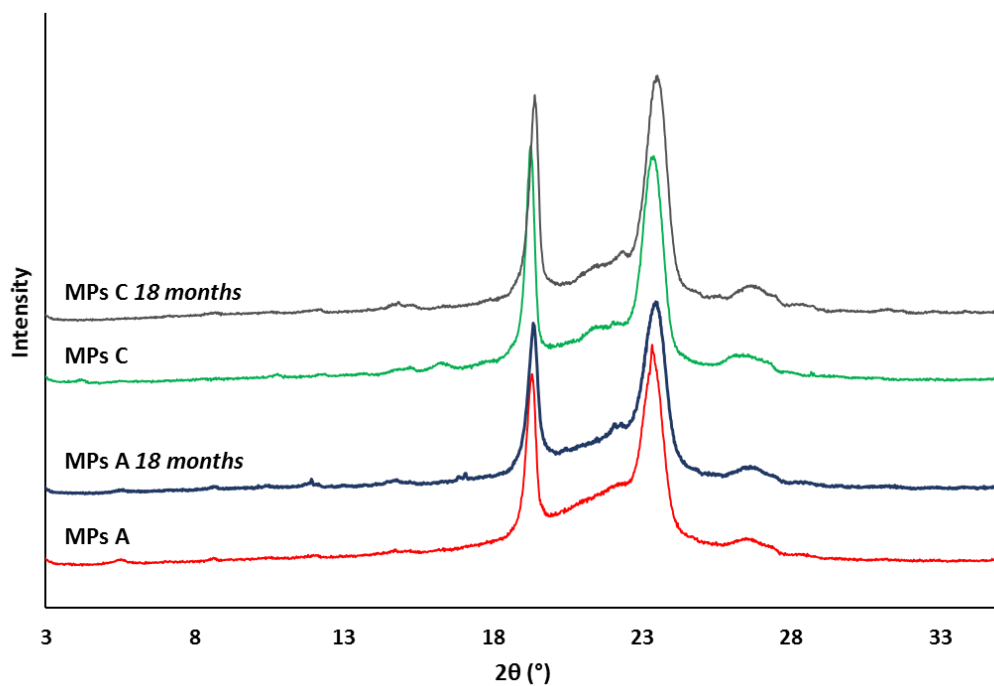
719 **Supporting information**

720



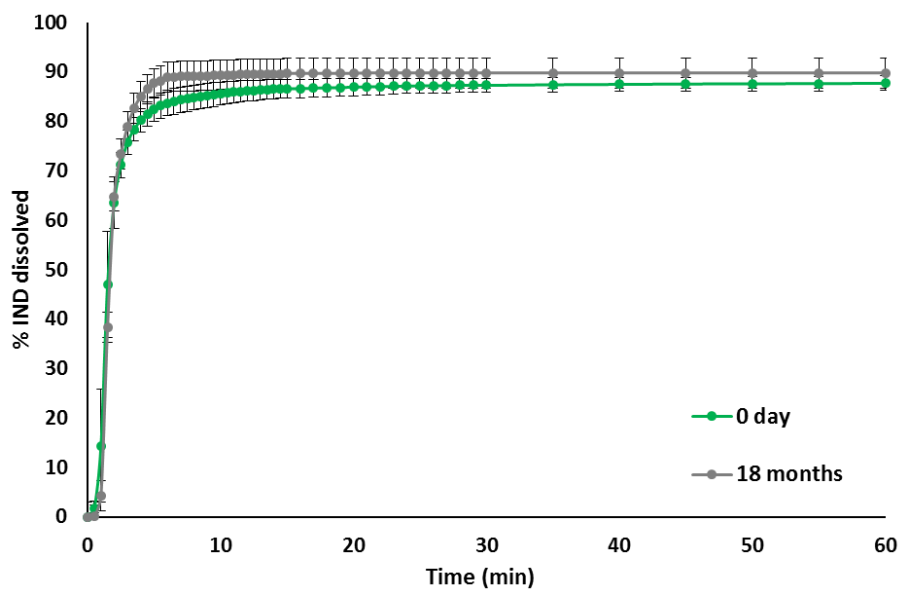
721

722 **Figure 1.** FT-IR spectra of MPs C immediately after preparation and after 18 months of storage.



723

724 **Figure 2.** Powder X-Ray diffractograms of MPs A and MPs C immediately after preparation and
725 after 18 months of storage.



726

727 **Figure 3.** Dissolution profiles of MPs C immediately after preparation and after 18 months of
728 storage in phosphate buffer pH 5.8. Data represents mean \pm SD ($n=3$).

729